ASH1 Gene Is a Specific Therapeutic Target for Lung Cancers with Neuroendocrine Features

Hirotaka Osada,[1] Yoshio Tatematsu,[1] Yasushi Yatabe,[2] Yoshitsugu Horio,[3] and Takashi Takahashi[4]

[1]Division of Molecular Oncology, Aichi Cancer Center Research Institute; [2]Department of Pathology and Molecular Diagnostics; [3]Division of Respiratory Tract, Aichi Cancer Center Hospital; and [4]Division of Molecular Carcinogenesis, Center for Neurological Diseases and Cancer, Nagoya University Graduate School of Medicine, Nagoya, Japan

Abstract

Lung cancers with neuroendocrine features are usually aggressive, although the underlying molecular mechanisms largely remain to be determined. The basic helix-loop-helix protein, achaete-scute complex-like 1/achaete-scute homologue 1 (ASH1), is expressed in normal fetal pulmonary neuroendocrine cells and lung cancers with neuroendocrine elements and is suggested to be involved in lung carcinogenesis. In the present study, we show inhibition of ASH1 expression by plasmid-based RNA interference (RNAi) to significantly suppress growth of lung cancer cells with ASH1 expression through G_2-M cell cycle arrest and accumulation of sub-G_1 populations, possibly linked to cleavage of caspase-9 and caspase-7. However, lung cancer cell lines without ASH1 expression and immortalized normal BEAS2B bronchial epithelial cells were not affected. The RNAi-resistant mutant ASH1 clearly induced rescue from G_2-M arrest, suggesting a target-specific effect of RNAi. An ASH1-RNAi adenovirus was also established and significantly inhibited not only *in vitro* cell proliferation but also *in vivo* xenograft growth of ASH1-positive NCI-H460 cells. Elevated levels of apoptosis were also observed in NCI-H460 xenografts with the ASH1-RNAi adenovirus. The present study therefore suggests that ASH1 plays a crucial role in lung cancer development and may be an effective therapeutic target in lung cancers with neuroendocrine features. (Cancer Res 2005; 65(23): 10680-5)

Introduction

Lung cancer is the leading cause of cancer-related death in Japan, as in many other economically well-developed countries. A better understanding of the molecular pathogenesis of this disease is thus urgently required for preventive or therapeutic breakthroughs to drastically reduce the number of deaths (1, 2). Based on their clinicopathologic characteristics, lung cancers are classified into two major groups, small cell lung cancers (SCLC) and non-SCLCs, the latter mainly comprising adenocarcinomas, squamous cell carcinomas, and large cell carcinomas. Immunohistochemical and molecular characterizations of lung cancers have shown the existence of a distinct subset of lung tumors with neuroendocrine features, which includes SCLCs, large cell carcinoma with neuroendocrine elements (LCNEC), and carcinoids. Although the LCNEC is usually differentiated from the SCLC, the two share several histologic features. Recently, a single group of high-grade neuroendocrine tumors (HGNET) was proposed for these two tumor types, based on the possible involvement of neuroendocrine differentiation in carcinogenesis (3). However, the underlying molecular mechanisms remain to be determined. Achaete-scute homologue 1 (ASH1) plays a crucial role in neural commitment and differentiation (4) and is also expressed in normal fetal pulmonary endocrine cells and lung cancers with neuroendocrine features (5, 6). Disruption of the *ASH1* gene also affects neuroendocrine differentiation, resulting in the loss of pulmonary neuroendocrine cells (7), in addition to defects of thyroid C cells, and adrenal medullary cells (8, 9). Constitutive expression of ASH1 promotes airway epithelial proliferation, and increase can result in the development of pulmonary hyperplasia and metaplasia. It also enhances tumorigenic potential with loss of p53 and Rb1 function induced by SV40 large T antigen, causing lung cancers with neuroendocrine features (10). Earlier experiments have thus clearly indicated an involvement of ASH1 in lung carcinogenesis. We here aimed at generating a better understanding of the role of ASH1 using an RNA interference (RNAi) for ASH1 transcripts. The ASH1-RNAi showed growth inhibitory effects *in vivo* and *in vitro* on lung cancer cell lines with ASH1 expression through induction of cell cycle arrest and apoptosis, providing support for the notion that ASH1 plays a crucial role in lung cancer development and may therefore be a promising therapeutic target for lung cancers with neuroendocrine features.

Materials and Methods

Cell culture and proliferation analysis. Cell lines were cultured as described previously (11) and transfected using Lipofectamine 2000 (Invitrogen, Carlsbad, CA). In proliferation assays, the numbers of transfected cells were measured with a colorimetric assay reagent, TetraColor One (Seikagaku, Tokyo, Japan), after selection with puromycin dihydrochloride (2 μg/mL; Sigma-Aldrich, St. Louis, MO) for 10 days.

RNA interference plasmid vectors and ASH1 constructs. For the construction of ASH1-RNAi plasmid, double-strand short hairpin RNA (shRNA) oligonucleotides containing the termination signal were inserted at the 3′ end of the U6 promoter. The shRNA oligonucleotides were as follows: CCCAAGCAAGTCAAGCGACAGTTCCAGCTGTCGCTTGACTTGCTTGGGCTTTTTTG for siASH1L1 (with the loop sequence containing a *Pvu*II site), CCCAAGCAAGTCAAGCGACAGCTTCCTGTCACTGTCGCTTGACTTGCTTGGGCTTTTTTG for siASH1L2 (containing the loop sequence for microRNA miR-23), and CGATATCTTTTTTG for the U6-blank.

The processing and expression of siRNA molecules with all ASH1-RNAi vectors were confirmed by Northern blot analysis using an oligonucleotide probe corresponding to the ASH1-RNAi site. For the ASH1 expression vector, full-length human ASH1 cDNA was amplified with reverse transcription-PCR (RT-PCR) and inserted into an expression vector, pcDNA3 (Invitrogen), together with the *myc* tag. The RNAi-resistant mutant ASH1 was constructed by PCR amplification using Pfu Turbo polymerase (Stratagene, La Jolla, CA) and a primer containing silent

Requests for reprints: Hirotaka Osada, Division of Molecular Oncology, Aichi Cancer Center Research Institute, 1-1 Kanokoden, Chikusa, Nagoya, 464-8681, Japan. Phone: 81-52-764-2993; Fax: 81-52-763-5233; E-mail: hosada@aichi-cc.jp.

doi:10.1158/0008-5472.CAN-05-1404

mutations: 5′-CACAAGTCAGCGCCGAAACAGGTTAAACGGCAACGCT-CGTCTTCG (mutated residues are underlined).

Immunoblots and reverse transcription-PCR. Expression of the transfected *ASH1* gene was studied with anti-*myc* tag antibody 9E10 (Santa Cruz Biotechnology, Santa Cruz, CA), whereas anti-ASH1 antibody (Santa Cruz Biotechnology) was used to detect endogenous ASH1 expression. For analysis of apoptosis, anti-cleaved caspase-3, cleaved caspase-7, cleaved caspase-8, caspase-9, and poly(ADP-ribose) polymerase (PARP) antibodies (Cell Signaling Technology, Beverly, MA) were used. RT-PCR was done using a one-step RT-PCR kit (Qiagen, Valencia, CA) according to the manufacturer's instructions.

Construction of the ASH1-RNA interference-adenovirus vector and experiments with the RNA interference-adenovirus. The ASH1-RNAi adenovirus was prepared using the Adeno-X Expression System (BD Clontech, Mountain View, CA; ref. 12). First, the cytomegalovirus promoter and SV40 polyadenylation signal in the mammalian expression cassette pShuttle plasmid were replaced by the U6 promoter and short hairpin oligonucleotides (siASH1L2 or U6-blank oligo). The replaced RNAi-Shuttle plasmid was then ligated into pAdeno-X plasmid. After *Pac*I digestion, the RNAi-adenoviral plasmid was transfected into HEK293 cells, and the recombinant RNAi-adenovirus was obtained. ASH1 siRNA expression was confirmed by Northern blot analysis of RNAs obtained from ASH1-RNAi-adenovirus–infected HEK293 cells (data not shown). RNAi effects on ASH1 expression were also detected after ASH1-RNAi adenovirus infection of HEK293 cells transfected with pcDNA3-ASH1 (data not shown). Viruses were propagated in HEK293 cells on a large scale, purified twice via ultracentrifugation in a cesium chloride gradient, and subjected to dialysis. Virus titers were determined by optical absorbance at $A_{260\ nm}$ (one $A_{260\ nm}$ unit = 10^{12} particles/mL) and by plaque assay. Titers determined by $A_{260\ nm}$ (i.e., viral particles) were used in all the experiments. Particle/plaque ratios normally fell between 30:1 and 100:1.

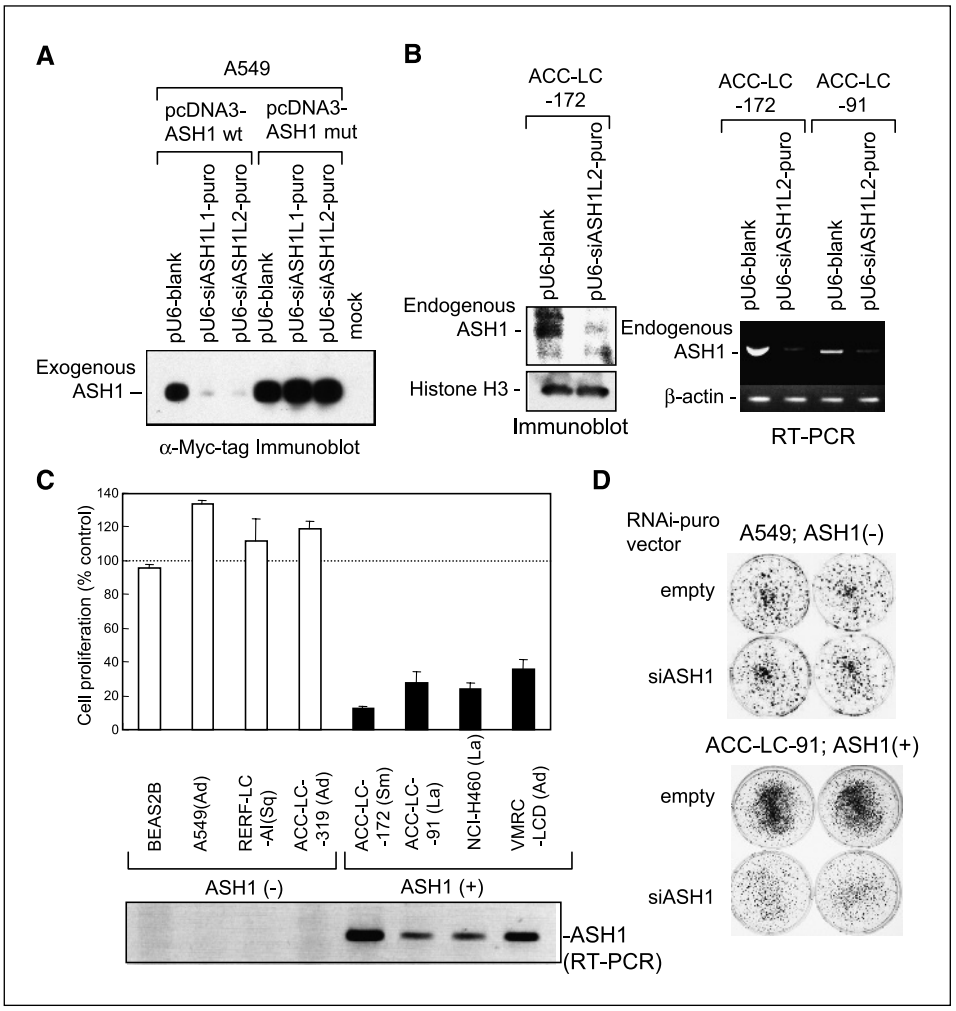

Figure 1. Inhibition of proliferation of lung cancer cell lines by ASH1-RNAi. *A,* immunoblot of ASH1 proteins. RNAi plasmid vectors were constructed by insertion of the U6 promoter (kindly provided by Dr. Ram Reddy, Baylor College of Medicine) 5′ upstream of the cytomegalovirus promoter, driving a puromycin-resistant gene (for pU6-siASH1L1/L2-puro). The ASH1-RNAi site was designed at 252 to 272 nucleotides of a 717-bp open reading frame, mainly based on the relaxed secondary structure of human ASH1 mRNA. A blast homology search did not indicate any gene with strong homology to the ASH1-RNAi site. A549 was transfected with each RNAi vector (pU6-blank and pU6-siASH1L1/L2-puro) along with the ASH1 expression vector (wild type and RNAi-resistant mutant). After puromycin selection, ASH1 expression was studied with immunoblotting. Significant reduction of expression of wild-type ASH1 protein was observed with both ASH1-RNAi vectors (pU6-siASH1L1/L2-puro) irrespective of the loop sequences. In contrast, the expression of silent mutant ASH1 (pcDNA3-ASH1 mut) was not affected. *B,* suppression of endogenous ASH1 expression by ASH-RNAi. The immunoblot with anti-ASH1 antibody clearly shows effective knockdown of endogenous ASH1 protein expression by the ASH1-RNAi vector in ACC-LC-172. RT-PCR analyses also showed knockdown of the endogenous ASH1 transcripts by RNAi in ACC-LC-172 and ACC-LC-91. *C,* inhibition of cell proliferation by ASH1-RNAi. Cells were plated into 3.5-cm culture dishes at 3×10^5 per dish and transfected with ASH1-RNAi vectors containing the puromycin-resistant gene. After transfection, cells were cultured in the presence of puromycin dihydrochloride (2 μg/mL; Sigma-Aldrich) for 10 days, and the cell number was then measured with a colorimetric assay reagent, TetraColor One (Seikagaku). *Columns,* % pU6-blank transfectant (% control). Lung cancer cells with ASH1 expression showed significant growth suppression by the ASH1-RNAi, although cell lines without ASH1 expression and the immortalized normal bronchial epithelial cell line BEAS2B were not affected. *D,* colonies of ACC-LC-91 [*ASH1 (+)*] and A549 [*ASH1 (−)*] cells in representative experiments shown by Giemsa staining. Note significant reduction of colony number only in the ACC-LC-91 case.

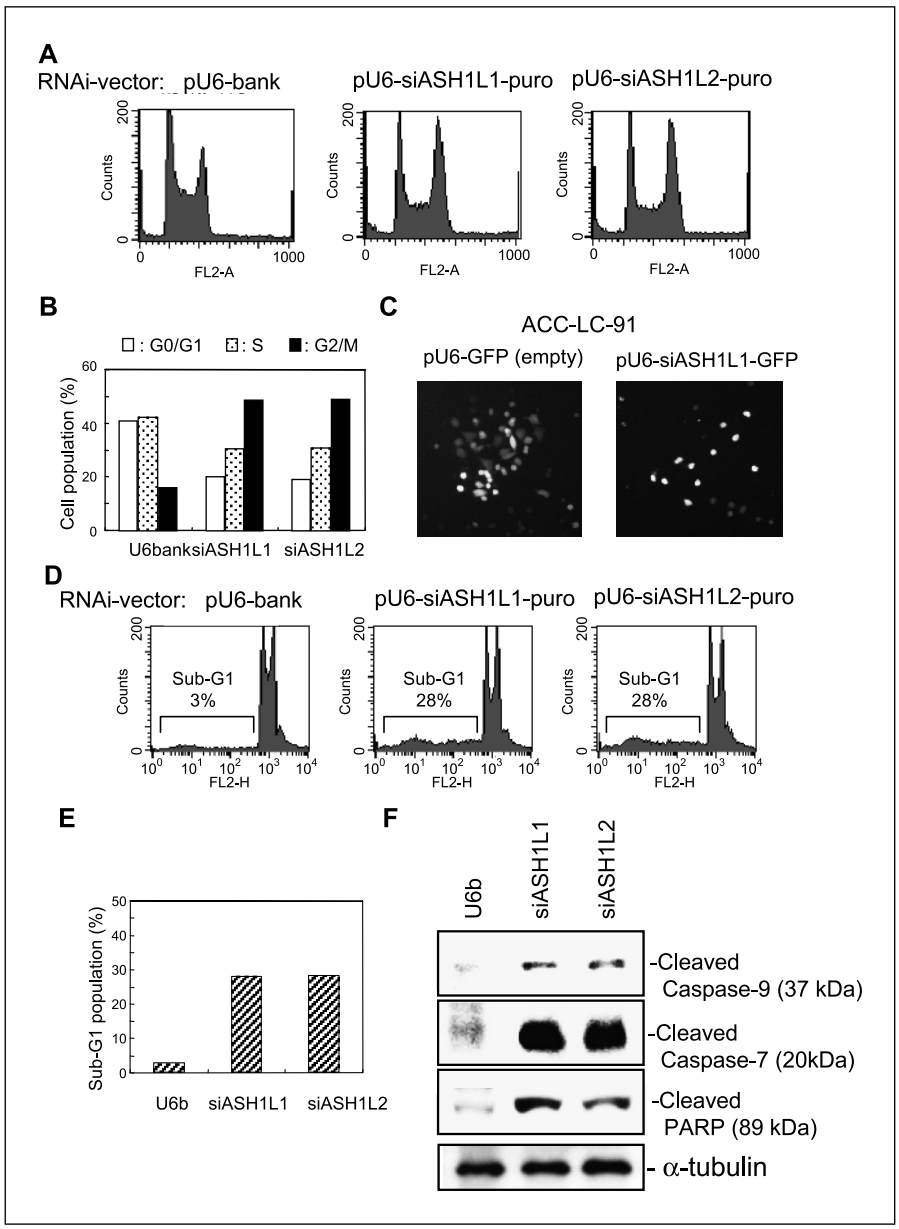

Figure 2. Induction of cell cycle arrest and apoptosis by ASH1-RNAi. Cells were transfected with RNAi vectors, selected with puromycin for 48 hours, cultured without puromycin for a further 24 hours, and harvested. Cell nuclei were stained with propidium iodide (Sigma-Aldrich), and then cellular DNA contents were measured with a flow cytometer FACSCalibur (Becton Dickinson, San Jose, CA) using CELLQuest and analyzed with ModFit (Becton Dickinson). *A-B,* fluorescence-activated cell sorting analysis of the cell cycle profile of ACC-LC-91 cells transfected with empty (pU6-blank) or ASH1-RNAi (pU6-siASH1L1/L2-puro) vectors. Both ASH1-RNAi vectors clearly induced G_2-M cell cycle arrest. *C,* proliferation of ACC-LC-91 cells transfected with the pU6-RNAi-GFP vector. In the pU6-RNAi-GFP vector, the U6 promoter and oligonucleotides were inserted 5′ upstream of the cytomegalovirus promoter driving the *GFP* gene. With empty pU6-GFP-transfected cells, GFP-positive cell clusters derived from multiple cell divisions were observed, whereas after pU6-siASH1-GFP transfection, GFP-positive cells are mainly solitary, suggesting lack of cell division of transfectants under puromycin-free conditions. *D-E,* accumulation of sub-G_1 populations with ASH1-RNAi (30% compared with only 3% with the empty-RNAi vector). *F,* Western blot analysis of components of the apoptotic signaling pathway. The initiator caspase (caspase-9) and the executioner caspase (caspase-7) were found to be cleaved in ACC-LC-91 cells after ASH1-RNAi induction. In addition, one of the substrates of executioner caspases (PARP) was also cleaved by activated caspases.

Infectivity of adenovirus particles for the lung cancer cell lines was confirmed using a β-galactosidase expressing adenovirus (Ad-LacZ; about 100 % by multiplicity of infection = 30). For *in vitro* experiments, NCI-H460 and A549 cells were plated onto 24-well plates at a density of 2×10^4 per well 1 day before virus infection. After infection, cell proliferation was determined using TetraColor One. For *in vivo* experiments, 5-week-old female severe combined immunodeficient (SCID) mice were purchased from Chubu Kagaku Shizai Co., Ltd. (Nagoya, Japan) and maintained under specific pathogen-free conditions. In the s.c. xenograft tumor model, 3×10^6 NCI-H460 cells or 1×10^7 ACC-LC-176 cells were s.c. inoculated into dorsal flanks to establish tumors. After tumors reached about 5 mm in diameter, mice were given two i.t. injections of 9×10^{10} viral particles at a volume of 100 μL per dose. One week after the first injection, mice were sacrificed, and tumors were harvested.

Results

The effects of suppressed ASH1 expression with ASH1-RNAi were studied in A549 cells on cotransfection of the ASH1 expression vector (pcDNA3-ASH1 wt) and the ASH1-RNAi vector (pU6-siASH1L1/L2-puro) after puromycin selection. The expression of wild-type ASH1 protein was significantly reduced by the ASH1-RNAi (Fig. 1*A*). In contrast, expression of the RNAi-resistant mutant ASH1 (pcDNA3-ASH1 mut) was not affected by the ASH1-RNAi construct (Fig. 1*A*). The knockdown of endogenous ASH1 expression was also studied in ACC-LC-172 and ACC-LC-91 expressing *ASH1* gene. The endogenous ASH1 expression was also significantly reduced by ASH1-RNAi at both protein and RNA levels (Fig. 1*B*).

To study the role of ASH1 in cell growth and carcinogenesis, cell proliferation assays were done with lung cancer cells transfected with pU6-siASH1L1-puro vectors. After puromycin selection, the number of stable transfectant colonies was assessed by colorimetric assay. Proliferation of lung cancer cells without ASH1 expression was not affected by ASH1-RNAi, whereas those with ASH1 expression showed significant growth suppression (Fig. 1*C*).

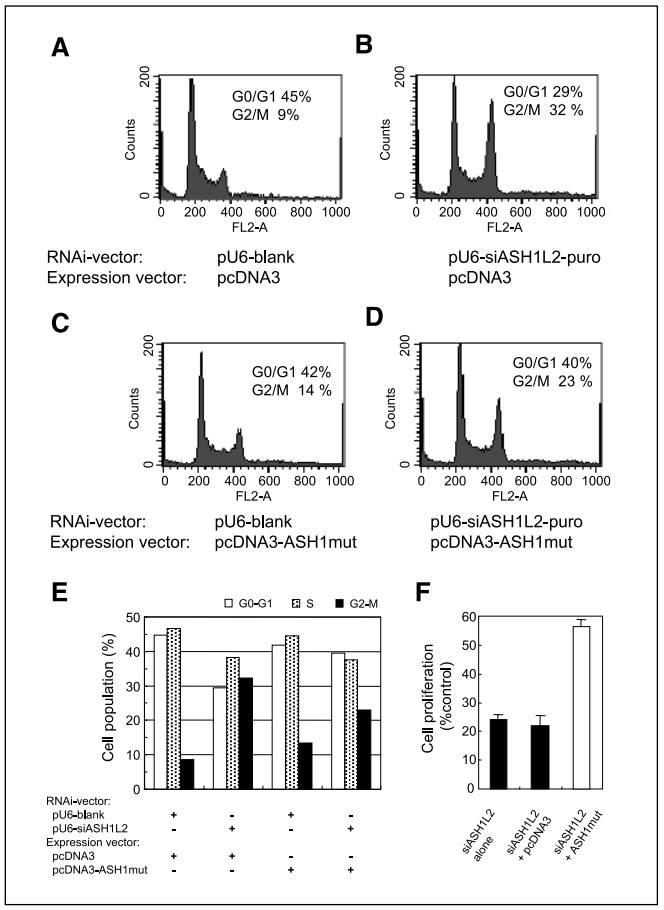

Figure 3. Rescue from ASH1-RNAi cell cycle arrest and growth inhibition by RNAi-resistant mutant ASH1. The cell cycle profile was analyzed as for Fig. 2. *A-D,* rescue of cell cycle arrest. ACC-LC-91 cells were cotransfected with the mutant ASH1 expression vector (*C* and *D*) or the empty expression vector (*A* and *B*) in addition to the ASH1-RNAi vector pU6-siASH1L2-puro (*B* and *D*) or the empty pU6-blank (*A* and *C*). Note reduction of G_1 and increase in G_2-M observed with the combination of pU6-siASH1L2-puro and empty pcDNA3 (*B*: G_1, 29% and G_2-M, 32%). In contrast, cotransfection of RNAi-resistant mutant ASH1 clearly reduced the G_2-M population and increased the G_1 population (*D*: G_1, 40% and G_2/M, 23%), suggesting the rescue from G_2-M arrest. *E,* graphical presentation of results of fluorescence-activated cell sorting analysis. *F,* rescue of growth inhibition. Similar to case illustrated in (*A-D*), ACC-LC-91 cells were cotransfected with the mutant ASH1 with the ASH1-RNAi vector and then treated with puromycin. Four days after transfection, the cell numbers were measured with a colorimetric assay. The mutant ASH1 indeed rescued the growth inhibition by ASH1-RNAi, indicating specificity for the growth inhibitory effect of ASH1-RNAi.

The immortalized normal bronchial epithelial cell line, BEAS2B, without ASH1 expression did not show growth suppression by ASH1-RNAi. Results of representative experiments with ACC-LC-91 [ASH1 (+)] and A549 [ASH1 (−)] are also shown. The ACC-LC-91 colony number was significantly reduced by ASH1-RNAi, whereas the A549 showed no difference between the empty vector and the ASH1-RNAi vector (Fig. 1*D*).

To understand the mechanisms of growth suppression by ASH1-RNAi, the ACC-LC-91 cell cycle profile after pU6-siASH1L1/L2-puro introduction was studied after puromycin selection. ASH1-RNAi clearly reduced the G_1- and S-phase populations with accumulation of cells in the G_2-M-phase (Fig. 2*A* and *B*). Cell proliferation was also studied using pU6-siASH1L1–green fluorescent protein (GFP) without puromycin selection to avoid the influence of this cytotoxic drug. Empty pU6-GFP vector transfection was associated with GFP-positive cell clusters, suggesting cell division of transfectants. In contrast, pU6-siASH1L1-GFP transfection resulted in mainly GFP strongly positive solitary cells (Fig. 2*C*).

In addition to the G_2-M arrest, ASH1-RNAi also caused accumulation of sub-G_1 populations (about 30% compared with 3% with the empty vector), implying induction of apoptotic cell death (Fig. 2*D* and *E*). Staining of unfixed cells with fluorescent dyes Hoechst33342 and propidium iodide showed apoptotic nuclear fragmentation only in ASH1-RNAi transfectants (data not shown). Activation of apoptotic signaling was also studied (Fig. 2*F*). The initiator caspase (caspase-9) and executioner caspase (caspase-7) were clearly activated by cleavage in ACC-LC-91 cells 48 hours after ASH1-RNAi induction. In addition, one of the substrates of executioner caspases (PARP) was also cleaved. Cleavage of caspase-8 or caspase-3, in contrast, was not clearly observed (data not shown).

To clarify the specificity of ASH1-RNAi effects, we did an experiment to rescue both cell cycle arrest (Fig. 3*A-E*) and growth inhibition (Fig. 3*F*) using an RNAi-resistant mutant ASH1 expression vector. ACC-LC-91 cells were cotransfected with the mutant ASH1 expression vector (or the empty expression vector) and the ASH1-RNAi vector (or the empty RNAi vector). The combination of ASH1-RNAi and the empty expression vector induced G_2-M arrest (G_1, 29% and G_2-M, 32%; Fig. 3*B*). In contrast, cotransfection of the RNAi-resistant mutant ASH1 clearly reduced the G_2-M population and increased the G_1 population (G_1, 40% and G_2-M, 23%; Fig. 3*D*), similar to the profile of the combination of mutant ASH1 and empty RNAi transfection (G_1, 42% and G_2-M, 14%; Fig. 3*C*). The cotransfection of mutant ASH1 also increased the viable cells 2.5-fold compared with the empty expression vector, indicating effective rescue of the growth inhibition by ASH1-RNAi (Fig. 3*F*). These rescue experiments implied that the cell cycle arrest and growth inhibitory effects of ASH1-RNAi are specifically induced by the inhibition of ASH1 expression itself.

Growth-inhibitory effects on ASH1-positive lung cancers were also studied with an adenovirus RNAi system, which might be applicable for *in vivo* therapeutic strategies. First, effects of ASH1-RNAi adenovirus infection on *in vitro* cell proliferation were ascertained. ASH1-positive NCI-H460 and ASH1-negative A549 cells were infected with the ASH1-RNAi-adenovirus (Ad-siASH1) or the empty RNAi-adenovirus (Ad-U6; Fig. 4*A* and *B*). The proliferation of ASH1-positive NCI-H460 cells was significantly inhibited only by the ASH1-RNAi-adenovirus and not by the empty RNAi-adenovirus (Fig. 4*A*). In contrast, cell growth of the ASH1-negative A549 was not affected by either Ad-siASH1 or Ad-U6 (Fig. 4*B*).

An *in vivo* therapeutic study was then done using lung cancer xenografts of NCI-H460 (ASH1 positive) or ACC-LC-176 (ASH1 negative) cells in SCID mice. Each adenovirus was injected directly into the xenograft tumors, and four animals per group were monitored for changes in tumor size before and after virus injection. In NCI-H460 xenografts, only treatment with Ad-siASH1 significantly suppressed tumor growth compared with Ad-U6. Before the first virus injection, there was no difference in estimated volumes of NCI-H460 tumors between the Ad-siASH1and Ad-U6 groups ($P = 0.71$). At sacrifice, the volume of NCI-H460 tumors in the Ad-siASH1 group was only 155 ± 46 mm^3, whereas that in the Ad-U6 group was 306 ± 29 mm^3 ($P = 0.0015$; Fig. 4*C*). The difference in NCI-H460 tumor weights between in the Ad-siASH1 and Ad-U6 groups was also statistically significant (112 ± 26 versus 240 ± 20 mg, $P = 0.0002$; Fig. 4*E*). In contrast, ACC-LC-176 tumors did not show any difference in either tumor volumes or weights

after Ad-siASH1 and Ad-U6 injections (Fig. 4*D* and *E*). Histopathologic study of NCI-H460 tumors treated with adenovirus showed significant differences in apoptosis between Ad-siASH1 and Ad-U6 treatments (Fig. 4*F*; $P < 0.0001$), suggesting that the ASH1-RNAi-adenovirus suppressed *in vivo* tumor growth at least partly through induction of apoptotic cell death, as the *in vitro* study.

Discussion

The present study showed clear suppression of ASH1 expression through ASH1-RNAi–induced G_2-M cell cycle arrest and apoptotic cell death. The induction of apoptosis was associated with activation of caspases, implying that ASH1 may play a role in the inhibitory regulation of cell death. Although the molecular mechanisms of induction of cell cycle arrest and apoptosis by ASH1-RNAi remain to be elucidated, the present findings imply a role for ASH1 in the regulation of cell proliferation and cell fate specifically in lung cancers with neuroendocrine features. Therefore, the results strongly indicate that ASH1 might be an effective therapeutic target for such lung cancers with ASH1 expression, notably aggressive and metastatic tumors with a poor prognosis. A recent report of the molecular consequences of ASH1-RNAi with large T antigen–induced prostate neuroendocrine cancer cells also suggested that ASH1 enhanced survival by inhibiting apoptosis in prostate neuroendocrine cancer cells (13). Further expression profiling analyses of ASH1-RNAi in lung neuroendocrine cancer cells seem warranted to generate better understanding of the molecular mechanisms underlying the present finding of anticancer effects of ASH1-RNAi.

For therapeutic strategies against molecular targets, specificity is critical for safety. The present rescue experiment using a RNAi-resistant ASH1 expression construct indicated that this was the

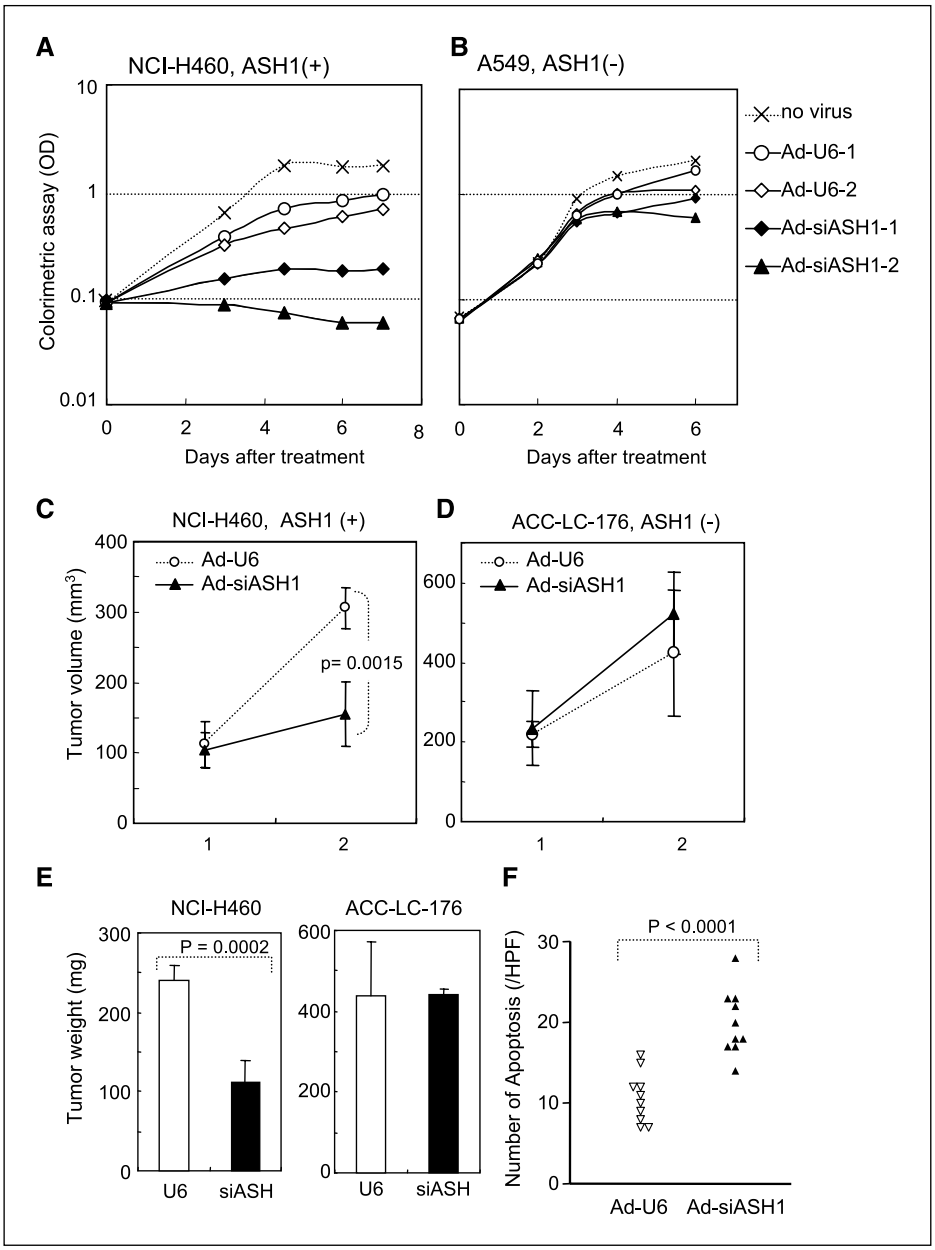

Figure 4. Growth inhibition and apoptosis induction by the ASH1-RNAi-adenovirus. *A-B,* inhibition of *in vitro* cell proliferation. *A,* proliferation of ASH1-positive NCI-H460 cells was significantly inhibited only by ASH1-RNAi-adenovirus (Ad-siASH1) and not by empty RNAi-adenovirus (Ad-U6). *B,* cell growth of the ASH1-negative A549 was not affected by either Ad-siASH1 or Ad-U6. Multiplicity of infection = 40 in Ad-U6-1 and Ad-siASH1-1; multiplicity of infection = 80 in Ad-U6-2 and Ad-siASH1-2. *C-E,* inhibition of *in vivo* tumor growth. Each adenovirus was injected directly into xenograft tumors of NCI-H460 (ASH1 positive) or ACC-LC-176 (ASH1 negative), and four animals per group were monitored for changes in tumor size. The tumor volumes (mm^3) were calculated (volume = length $\times$ width^2 $\times$ 0.52) just before the first virus injection (*1*) and at sacrifice 1 week after the first injection (*2*). *C,* in NCI-H460 xenografts, injection of Ad-siASH1 significantly suppressed tumor growth compared with Ad-U6 ($P = 0.0015$), there being no differences before the injection between these two groups ($P = 0.71$). *D,* in contrast, ACC-LC-176 tumors did not show any differences in the tumor volumes between the Ad-siASH1 and Ad-U6 injections. *E,* measured weights (mg) of tumors from the sacrificed mice. Similar to (*C*), in NCI-H460 xenografts, injection of Ad-siASH1 significantly suppressed tumor growth compared with Ad-U6 (Ad-siASH1: 112 $\pm$ 26 mg versus Ad-U6: 240 $\pm$ 20 mg; $P = 0.0002$). In contrast, ACC-LC-176 tumors again did not show any differences between the Ad-siASH1 and Ad-U6 injections. *F,* apoptosis induction in NCI-H460 tumors by the ASH1-RNAi-adenovirus. On histopathologic study of NCI-H460 tumors treated with adenovirus, apoptotic cells were observed in Ad-siASH1-injected tumors more frequently than in Ad-U6-injected tumors ($P < 0.0001$). Individual counts for apoptotic cells in each HPF with (▽) Ad-U6 and (▲) Ad-siASH1 injections.

case for the ASH1-RNAi regarding cell cycle arrest and growth inhibition, with no involvement of "off-target effects." ASH1 disruption is known to induce developmental defects of olfactory and autonomic neurons, without any adverse influence on the central nervous system (4). However, abnormalities specific to pulmonary neuroendocrine cells were noted, with no effects on autonomic neurons or non-neuroendocrine airway epithelial cells in the lung. Therefore, the lung delivery of ASH1-RNAi (oligonucleotides or adenovirus) may allow a specific therapeutic strategy for lung cancers with neuroendocrine features.

Several reports have indicated functional interactions between ASH1 and Notch-Hes1 signaling, suggesting that they mutually exclusively regulate the differentiation of airway common precursors for neuroendocrine and Clara cells (5, 6, 14). Notch1 induces rapid degradation of the hASH1 protein and G_1 cell cycle arrest of SCLC cell lines associated with p21Cip1 and p27Kip1 induction (15). Our preliminary studies showed no clear induction of either p21Cip1 or p27Kip1 in ASH1-RNAi–treated ACC-LC-91 (data not shown), suggesting that the other mechanisms might be involved in the G_2-M arrest by ASH1-RNAi.

Other possible functions of the *ASH1* gene might be related to autocrine/paracrine signaling of growth factors. Autocrine signals of neuroendocrine regulatory peptides (e.g., bombesin/gastrin-releasing peptide) are prominent in SCLCs (1), and signaling pathways of neurotrophins and their receptors (*Trk* genes) have been reported to be involved in the regulation of lung cancer cell growth (16). In addition, one neurotrophin receptor, TrkB, is known as an inhibitor of anoikis (17). Thus, autocrine/paracrine loops might be associated with ASH1 expression and inhibited by ASH1-RNAi, resulting in the induction of cell death. Expression profiling analysis of ASH1-RNAi will provide important information on functions of the *ASH1* gene and its role in the development of lung cancers with neuroendocrine features.

SCLC is an aggressive and highly metastatic tumor. Although usually responsive to chemotherapy, recurrent tumors almost always develop in a chemotherapy- resistant form. In addition, little is known about the chemotherapy-responsiveness of LCNECs. Therefore, an emphasis on therapeutic strategy is necessary for lung cancers with neuroendocrine features. The present study provides a basis for further analysis of the molecular effect of the ASH1-RNAi, which will hopefully facilitate establishment of novel and potent therapeutics for HGNETs.

Acknowledgments

Received 4/25/2005; revised 8/29/2005; accepted 9/29/2005.

Grant support: Ministry of Education, Culture, Sports, Science and Technology of Japan grants-in-aid for Scientific Research on Priority Areas and Scientific Research (C); grant-in-aid for the Third Term Comprehensive Ten-year Strategy for Cancer Control; and Ministry of Health, Labour, and Welfare, Japan grant-in-aid for Cancer Research.

The costs of publication of this article were defrayed in part by the payment of page charges. This article must therefore be hereby marked *advertisement* in accordance with 18 U.S.C. Section 1734 solely to indicate this fact.

References

1. Wistuba II, Gazdar AF, Minna JD. Molecular genetics of small cell lung carcinoma. Semin Oncol 2001;28:3–13.
2. Osada H, Takahashi T. Genetic alterations of multiple tumor suppressors and oncogenes in the carcinogenesis and progression of lung cancer. Oncogene 2002;21:7421–34.
3. Jones MH, Virtanen C, Honjoh D, et al. Two prognostically significant subtypes of high-grade lung neuroendocrine tumours independent of small-cell and large-cell neuroendocrine carcinomas identified by gene expression profiles. Lancet 2004;363:775–81.
4. Guillemot F, Lo LC, Johnson JE, Auerbach A, Anderson DJ, Joyner AL. Mammalian achaete-scute homolog 1 is required for the early development of olfactory and autonomic neurons. Cell 1993;75:463–76.
5. Ito T, Udaka N, Okudela K, Yazawa T, Kitamura H. Mechanisms of neuroendocrine differentiation in pulmonary neuroendocrine cells and small cell carcinoma. Endocr Pathol 2003;14:133–9.
6. Ball DW. Achaete-scute homolog-1 and Notch in lung neuroendocrine development and cancer. Cancer Lett 2004;204:159–69.
7. Borges M, Linnoila RI, van de Velde HJ, et al. An achaete-scute homologue essential for neuroendocrine differentiation in the lung. Nature 1997;386:852–5.
8. Lanigan TM, DeRaad SK, Russo AF. Requirement of the MASH-1 transcription factor for neuroendocrine differentiation of thyroid C cells. J Neurobiol 1998;34:126–34.
9. Huber K, Bruhl B, Guillemot F, Olson EN, Ernsberger U, Unsicker K. Development of chromaffin cells depends on MASH1 function. Development 2002;129:4729–38.
10. Linnoila RI, Zhao B, DeMayo JL, et al. Constitutive achaete-scute homologue-1 promotes airway dysplasia and lung neuroendocrine tumors in transgenic mice. Cancer Res 2000;60:4005–9.
11. Osada H, Tatematsu Y, Masuda A, et al. Heterogeneous transforming growth factor (TGF)-β unresponsiveness and loss of TGF-β receptor type II expression caused by histone deacetylation in lung cancer cell lines. Cancer Res 2001;61:8331–9.
12. Horio Y, Hasegawa Y, Sekido Y, Takahashi M, Roth JA, Shimokata K. Synergistic effects of adenovirus expressing wild-type p53 on chemosensitivity of non-small cell lung cancer cells. Cancer Gene Ther 2000;7:537–44.
13. Hu Y, Wang T, Stormo GD, Gordon JI. RNA interference of achaete-scute homolog 1 in mouse prostate neuroendocrine cells reveals its gene targets and DNA binding sites. Proc Natl Acad Sci U S A 2004;101:5559–64.
14. Reynolds SD, Hong KU, Giangreco A, et al. Conditional Clara cell ablation reveals a self-renewing progenitor function of pulmonary neuroendocrine cells. Am J Physiol Lung Cell Mol Physiol 2000;278:L1256–63.
15. Sriuranpong V, Borges MW, Ravi RK, et al. Notch signaling induces cell cycle arrest in small cell lung cancer cells. Cancer Res 2001;61:3200–5.
16. Oelmann E, Sreter L, Schuller I, et al. Nerve growth factor stimulates clonal growth of human lung cancer cell lines and a human glioblastoma cell line expressing high-affinity nerve growth factor binding sites involving tyrosine kinase signaling. Cancer Res 1995;55:2212–9.
17. Geiger TR, Peeper DS. The neurotrophic receptor TrkB in anoikis resistance and metastasis: a perspective. Cancer Res 2005;65:7033–6.

ASH1 Gene Is a Specific Therapeutic Target for Lung Cancers with Neuroendocrine Features

Hirotaka Osada, Yoshio Tatematsu, Yasushi Yatabe, et al.

Cancer Res 2005;65:10680-10685.